**Table 3 Equilateral octagonal plates subjected to uniform compression in the $x$ direction**

| Strips × elements | 4×4 | 5×4 | 5×5 | 5×6 | 6×5 |
|---|---|---|---|---|---|
| Buckling factors | 11.524 | 6.397 | 4.534 | 4.532 | 4.526 |

**Table 4 Twelve-sided plates with uniform compression in the $x$ direction**

| Strips × elements | 4×4 | 4×5 | 5×4 | 5×5 | 5×6 |
|---|---|---|---|---|---|
| Buckling factors | 5.579 | 4.907 | 4.677 | 4.348 | 4.334 |

**Table 5 Sixteen-sided plates subjected to uniform compression in the $x$ direction**

| Strips × elements | 4×4 | 4×5 | 5×5 | 5×6 | 6×6 |
|---|---|---|---|---|---|
| Buckling factors | 5.297 | 4.605 | 4.292 | 4.277 | 4.272 |

**Table 6 Buckling factors of equilateral polygons**

| No. of sides of polygon | 8 | 12 | 16 | 20 |
|---|---|---|---|---|
| Buckling factors | 4.526 | 4.334 | 4.272 | 4.208 |

2) For a simply supported trapezoidal plate under uniformly compressive loading in the $x$-direction, the finest division used is a 4 strip × 11 element model on one-half of the trapezoidal plate. The plate is isosceles with a height of (a), the parallel sides measure ($a$ and $3a$), and the height/thickness ratio ($a/t$) is 100. The average width of ($2a$) is used in lieu of ($a$) in Eq. (14). It is subjected to uniform normal compression along the parallel sides. Buckling factors (with increasing strips and elements) are shown in Table 2. The buckling factor $\lambda_b$ approaches 6.1.

3)The buckling factors shown in Table 3 are for simply supported equilateral octagonal plates under compressive loading in the $x$ direction (Fig. 1).

4) The results of a simply supported, equilateral, 12-sided plate are investigated. The results are shown in Table 4.

5) The buckling factors of a simply supported, equilateral, 16-sided polygon plate are shown in Table 5.

6) Table 6 lists the buckling factors for different equilateral polygons, including the circle (a polygon approximated by 20 sides). It can be seen that the buckling factor of equilateral polygons approaches that of a circle as the number of sides increase.

## Summary

It can be seen from illustrative examples and tables that the proposed method converges rapidly and accurately when compared with known solutions. The computational labor for the proposed method is about 2 to 3 times less than that used by finite element programs of similar accuracy.[6] Based on the authors' experience, more elements (compared with number of strips) give better accuracy.

## References

[1]Timoshenko, S.P. and Gere, J., *Theory of Elastic Stability*, 2nd Ed., McGraw-Hill Book Co., New York, Vol. 92, 1961.

[2]Kapur, K.K. and Hartz, B.J., "Stability of Plates Using the Finite Element Method," *ASCE Journal of Engineering Mechanics Division*, April 1966, pp. 177-195.

[3]Anderson, R.G., Irons, B.M. and Zienkiewicz, O.C., "Vibration and Stability of Plates Using Finite Elements, *International Journal of Solid Structures*, Vol.4, 1968, pp. 1031-1055.

[4]Cheung, Y.K., "Finite Strip Method in the Analysis of Elastic Plates with Two Opposite Simply Supported Ends, *Proceedings of the Institute of Civil Engineering*, Vol. 40, May 1968, p. 17.

[5]Cheung, Y.K., *Finite Strip Method in Structural Analysis*, Pergamon Press, Oxford, England, 1976.

[6]Yang, H.Y. and Chong, K.P., "Finite Strip Method with $x$-Spline Functions," *Computers and Structures*, Vol. 18, No. 1, 1984, pp. 127-132.

[7]Chen, J.L. and Chong, K.P., "Vibration of Irregular Plates by Finite Strip Method with Spline Functions," *Proceedings of 5th ASCE–EMD Specialty Conference*, Laramie, WY, Aug. 1984, pp. 256-260.

[8]Cheung, Y.K., Tham, L.G., and Chong, K.P., "Buckling of Sandwich Plate by Finite Layer Method," *Computers and Structures*, Vol. 15, No.2, 1982, pp. 131-134.

[9]Clenshaw, C.W. and Negus, B., "The Cubic $x$-Spline and Its Applications," *Journal Institute of Mathematics and Applications*, Vol. 22, 1978, pp. 109-119.

[10]Moler, C.B. and Stewart, G.W., "An Algorithm for Generalized Matrix Eigenvalue Problems," *Journal of Numerical Analysis*, Vol. 10, 1973, pp. 241-256.

[11]Zienkiewicz, O.C. and Cheung, Y.K., *The Finite Element Method in Structural and Continuum Mechanics*, McGraw-Hill Book Co., New York, 1967.

[12]Chen, J.L., "Modified Finite Strip Method with Spline Functions," *Ph.D. Thesis*, University of Wyoming, 1985, directed by K.P. Chong.

[13]Vandergraft, J.S., *Introduction to Numerical Computations*, 4th Ed., John Wiley & Sons, New York, 1974.

# Vibrations of Infinitely Long Cylindrical Shells of Noncircular Cross Section

V. K. Koumousis*
*Athens, Greece*
and
A. E. Armenakas†
*Polytechnic University of New York, New York*

## Displacement Equations of Motion

CONSIDER a thin-walled, closed, infinitely long cylindrical shell having a noncircular cross section of constant thickness $h$ and made of an isotropic, linearly elastic material. The shell is referred to a right-hand system of orthogonal curvilinear coordinates $x^*$, $s^*$, and $z$. $x^*$ is measured along the axis of the shell, $s^*$ along the curve formed by the intersection of the plane normal to the axis of the shell and its middle surface, and $z$ inward along the direction perpendicular to the middle surface of the shell.

The $x^*$, $s^*$ coordinates and the radius of curvature $r^*$ of the cross section of the shell are nondimensionalized with

Received March 4, 1985; revision received May 15, 1985. 

*Consulting Engineer.

†Professor of Aerospace Engineering. Associate Fellow AIAA.

respect to the radius $r_0$ of a circle whose perimeter is equal to that of the noncircular cross section of the shell. That is, $x=x^*/r_0$, $s=s^*/r_0$, and $r=r^*/r_0$.

The displacement equations of motion of a Flügge-type theory for cylindrical shells of any cross section are

$$\begin{bmatrix} L_{11} & L_{12} & L_{13} \\ L_{21} & L_{22} & L_{23} \\ L_{31} & L_{32} & L_{33} \end{bmatrix} \begin{bmatrix} u(x,s,t) \\ v(x,s,t) \\ w(x,s,t) \end{bmatrix} = \begin{bmatrix} 0 \\ 0 \\ 0 \end{bmatrix} \tag{1}$$

where $u$, $v$, $w$ are the longitudinal, circumferential, and radial components of displacement, respectively. For the Flügge-type theory, the operators $L_{ij}$, $i, j=1,2,3$ are given in Ref. 1.

## Harmonic Oscillations of Infinitely Long Cylindrical Shells

An infinitely long cylindrical shell can vibrate in modes having any axial wavelength. Its components of displacement can be expanded in a complete double Fourier series in the axial and circumferential variables and, thus, the solution for harmonic oscillations can be assumed as

$$u(x,s,t) = e^{i\omega t}[\cos\lambda x U(s) + \sin\lambda x \bar{U}(s)]$$

$$v(x,s,t) = e^{i\omega t}[\sin\lambda x V(s) - \cos\lambda x \bar{V}(s)]$$

$$w(x,s,t) = e^{i\omega t}[\sin\lambda x W(s) - \cos\lambda x \bar{W}(s)] \tag{2}$$

where

$$U(s) = \sum_{n=0,1,2}^{\infty} (A_n \cos ns + B_n \sin ns)$$

$$V(s) = \sum_{n=0,1,2}^{\infty} (C_n \cos ns + D_n \sin ns)$$

$$W(s) = \sum_{n=0,1,2}^{\infty} (E_n \cos ns + F_n \sin ns)$$

$$\bar{U}(s) = \sum_{n=0,1,2}^{\infty} (\bar{A}_n \cos ns + \bar{B}_n \sin ns)$$

$$\bar{V}(s) = \sum_{n=0,1,2}^{\infty} (\bar{C}_n \cos ns + \bar{D}_n \sin ns)$$

$$\bar{W}(s) = \sum_{n=0,1,2}^{\infty} (\bar{E}_n \cos ns + \bar{F}_n \sin ns) \tag{3}$$

with $B_0 \equiv \bar{B}_0 \equiv D_0 \equiv \bar{D}_0 \equiv F_0 \equiv \bar{F}_0 \equiv 0$.

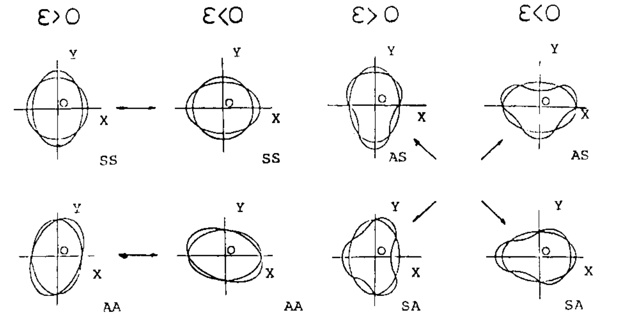


**Fig. 1 Representation of the different types of modes of oval cylindrical shells.**

In Eq. (2), $\omega$ is the circular frequency of the vibrations, $L$ is the given half axial wavelength, and

$$\lambda = \pi r_0/L \tag{4}$$

Substitution of the components of displacement [Eqs. (2)] into the equations of motion (1) results in the following relations:

$$P\cos\lambda x + \bar{P}\sin\lambda x = 0$$

$$Q\sin\lambda x + \bar{Q}\cos\lambda x = 0$$

$$R\sin\lambda x + \bar{R}\cos\lambda x = 0 \tag{5}$$

where

$$P = -\left(\frac{1-\nu}{2}\right)\left(1+\frac{k}{r^2}\right)U''(s) + k\left(\frac{1-\nu}{2}\right)\frac{2r'}{r^3}U'(s)$$
$$+(\lambda^2-\Omega^2)U(s) - \left(\frac{1+\nu}{2}\right)\lambda V'(s) + k\left(\frac{1-\nu}{2}\right)\frac{\lambda}{r}W''(s)$$
$$-k\left(\frac{1-\nu}{2}\right)\lambda\frac{r'}{r^2}W'(s) + \frac{1}{r}(\nu\lambda + k\lambda^3)W \tag{6a}$$

$$Q = \left(\frac{1+\nu}{2}\right)\lambda U'(s) - V''(s) + \left[\left(\frac{1-\nu}{2}\right)\lambda^2 + k\left(\frac{r'}{r^2}\right)^2\right.$$
$$\left.+3k\left(\frac{1-\nu}{2}\right)\frac{\lambda^2}{r^2} - \Omega^2\right]V(s) - \frac{kr'}{r^2}W''(s)$$
$$+\frac{1}{r}\left[1+k\left(\frac{3-\nu}{2}\right)\lambda^2\right]W'(s) - \left(\frac{r'}{r^2} - \frac{kr'}{r^4}\right)W(s) \tag{6b}$$

$$R = k\left(\frac{1-\nu}{2}\right)\frac{\lambda}{r}U''(s) - k\left(\frac{1-\nu}{2}\right)\lambda\frac{r'}{r^2}U'(s)$$
$$+\left(\frac{k\lambda^3}{r} + \frac{\nu\lambda}{r}\right)U(s) - \frac{kr'}{r^2}V''(s)$$
$$-\left[k\left(\frac{3-\nu}{2}\right)\frac{\lambda^2}{r} + \frac{1}{r} + 2k\left(\frac{r'}{r^2}\right)'\right]V'(s)$$
$$+\left[k\left(\frac{3-\nu}{2}\right)\lambda^2\frac{r'}{r^2} - k\left(\frac{r'}{r^2}\right)'' - \frac{kr'}{r}\right]V(s)$$
$$+kW''''(s) + \left(\frac{2k}{r^2} - 2k\lambda^2\right)W''(s) - 4\frac{kr'}{r^3}W'(s)$$
$$+\left[k\lambda^4 + 2k\left(\frac{r}{r^3}\right) + \frac{k}{r^4} + \frac{1}{r^2} - \Omega^2\right]W(s) \tag{6c}$$

Moreover, $\bar{P}$, $\bar{Q}$, $\bar{R}$ are obtained from Eqs. (6) by substituting $\bar{U}$, $\bar{V}$, $\bar{W}$ for $U$, $V$, $W$.

In Eqs. (6), the prime denotes differentiation with respect to $s$, $\Omega^2$ is the nondimensional frequency, and $k$ is the nondimensional thickness parameter defined as

$$\Omega^2 = \left(\frac{1-\nu^2}{E}\right)\rho r_0^2\omega^2, \quad k = \frac{h^2}{12r_0^2} \tag{7}$$

Equations (5) are valid for any value of $x$ and, consequently, the coefficients of the linearly independent sine and cosine terms must vanish, resulting in the following two systems of ordinary linear differential equations with variable coefficients:

$$P=Q=R=0 \text{ and } \bar{P}=\bar{Q}=\bar{R}=0 \tag{8}$$

Inasmuch as the solutions of both systems of Eqs. (8) must satisfy the same periodicity conditions, we have

$$\bar{U}(s)=c_1 U(s), \quad \bar{V}(s)=c_1 V(s), \quad \bar{W}(s)=c_1 W(s) \tag{9}$$

Using Eqs. (9), it can be shown that Eqs. (2) assume the following form:

$$u(x,s,t)=e^{i\omega t}\cos(\lambda x-x_0)U(s)$$

$$v(x,s,t)=e^{i\omega t}\sin(\lambda x-x_0)V(s)$$

$$w(x,s,t)=e^{i\omega t}\sin(\lambda x-x_0)W(s) \tag{10}$$

Comparing the solution of Eqs. (10) to that of simply supported cylindrical shells,[1] it is apparent that:

1) The frequencies and mode shapes of an infinitely long cylindrical shell vibrating in modes with finite axial wavelength $2L/m\,(m\neq 0)$ are identical to those of a simply supported shell of the same cross section and length $L$ vibrating in modes with axial wavenumber $m$.

2) For $m=0$, the modes of vibration of simply supported shells become purely longitudinal.[1] Plane strain modes cannot be excited in simply supported shells.

3) In the limit as $L\to\infty\,(m=0)$, the modes of vibration of an infinitely long shell uncouple into purely longitudinal modes ($u\neq 0$, $v=w=0$) and plane strain modes ($u=0$, $v\neq 0$, $w\neq 0$). In this case, Eqs. (5) reduce to

$$P=0 \tag{11}$$

$$\bar{Q}=\bar{R}=0 \tag{12}$$

The frequencies of purely longitudinal modes are obtained from Eq. (11) and are identical to those of the corresponding modes of simply supported shells. The frequencies of plane strain modes are obtained from Eq. (12).

To the order of accuracy of the Donnell, Love, and Sanders theories, the frequency equation for the purely longitudinal modes reduces to

$$\cos 2\pi\beta = 1 \tag{13}$$

where $\beta^2=2\Omega_n^2/(1-\nu)$. Therefore, their eigenfrequencies and mode shapes are

$$\Omega_n = n\sqrt{\left(\frac{1-\nu}{2}\right)}, \quad U^{(n)}(s)=(C_{1n}\sin ns + C_{2n}\cos ns) \tag{14}$$

That is, to the order of accuracy of the Donnell, Love, and Sanders theories, the frequencies and mode shapes of the purely longitudinal modes are independent of the geometry of the cross section of the shell.

## Frequencies of Purely Longitudinal and Plane Strain Modes of Infinitely Long Oval Cylindrical Shells

The radius of curvature of an oval cross section is given as[1]

$$1/r(s)=1+\epsilon\cos 2s \tag{15}$$

where $\epsilon$ is the ovality parameter $|\epsilon|<1$. Substituting Eq. (15) into Eqs. (11) and (12) and taking the limit as $L\to\infty$, the following homogeneous equations are obtained:

$$\sum_{n=0,1,2}^{\infty} G_n^{(1)}\cos ns + \sum_{n=1,2,3}^{\infty} H_n^{(1)}\sin ns = 0 \tag{16}$$

$$\sum_{n=0,1,2}^{\infty} G_n^{(2)}\sin ns + \sum_{n=0,1,2}^{\infty} H_n^{(2)}\cos ns = 0 \tag{17a}$$

$$\sum_{n=0,1,2}^{\infty} G_n^{(3)}\cos ns + \sum_{n=1,2,3}^{\infty} H_n^{(3)}\sin ns = 0 \tag{17b}$$

where

$$G_n^{(1)}=(\alpha_1-\Omega^2)A_n+\alpha_2 A_{n-2}+\alpha_3 A_{n+2}+\alpha_4 A_{n-4}+\alpha_5 A_{n+4} \tag{18}$$

Table 1 Frequencies of symmetric modes of infinitely long oval cylindrical shells, $r_0/h=20$, $\nu=0.3$

| | | $\epsilon=0$ | | | $\epsilon=0.6$ | | | $\epsilon=0.1$ | | |
|---|---|---|---|---|---|---|---|---|---|---|
| | | | Plane strain | | | Plane strain | | | Plane strain | |
| Theory | $n$ | Axial | Lower | Higher | Axial | Lower | Higher | Axial | Lower | Higher |
| Donnell | 0 | 0.0 | 0.0 | 1.000000 | 0.0 | 0.0 | 1.005629 | 0.0 | 0.0 | 1.036201 |
| Love | 0 | 0.0 | 0.0 | 1.000000 | 0.0 | 0.0 | 1.005713 | 0.0 | 0.0 | 1.036447 |
| Sanders | 0 | 0.0 | 0.0 | 1.000000 | 0.0 | (i)[a] | 1.005646 | 0.0 | (i) | 1.036538 |
| Flügge | 0 | 0.0 | 0.0 | 1.000104 | 0.0 | 0.0 | 1.005738 | 0.0 | 0.0 | 1.036619 |
| Donnell | 1 | 0.591608 | 0.010205 | 1.414250 | 0.591608 | 0.008782 | 1.648208 | 0.591608 | 0.007969 | 1.812226 |
| Love | 1 | 0.591608 | 0.014434 | 1.414287 | 0.591608 | 0.021781 | 1.648222 | 0.591608 | 0.033037 | 1.812257 |
| Sanders | 1 | 0.591608 | 0.0 | 1.414361 | 0.591608 | (i) | 1.648244 | 0.591608 | (i) | 1.812284 |
| Flügge | 1 | 0.591669 | 0.0 | 1.414214 | 0.591643 | 0.0 | 1.648208 | 0.591638 | 0.0 | 1.812356 |
| Donnell | 2 | 1.183216 | 0.051636 | 2.236217 | 1.183216 | 0.049609 | 2.325569 | 1.183216 | 0.045951 | 2.465903 |
| Love | 2 | 1.183216 | 0.053232 | 2.136366 | 1.183216 | 0.052478 | 2.325708 | 1.183216 | 0.049186 | 2.466031 |
| Sanders | 2 | 1.183216 | 0.038719 | 2.236664 | 1.183216 | 0.037823 | 2.326027 | 1.183216 | 0.037113 | 2.466370 |
| Flügge | 2 | 1.183339 | 0.038728 | 2.236152 | 1.183350 | 0.039071 | 2.325580 | 1.183370 | 0.039474 | 2.466049 |
| Donnell | 3 | 1.774824 | 0.123227 | 3.162545 | 1.774824 | 0.121744 | 3.197383 | 1.774824 | 0.119930 | 3.263898 |
| Love | 3 | 1.774824 | 0.124000 | 3.162811 | 1.774824 | 0.122824 | 3.197675 | 1.774824 | 0.121179 | 3.264227 |
| Sanders | 3 | 1.774824 | 0.109507 | 3.163346 | 1.774824 | 0.107158 | 3.198302 | 1.774824 | 0.104517 | 3.264994 |
| Flügge | 3 | 1.775009 | 0.109537 | 3.162489 | 1.775042 | 0.107317 | 3.197371 | 1.775101 | 0.104867 | 3.262966 |
| Donnell | 4 | 2.366432 | 0.224024 | 4.123487 | 2.366432 | 0.221895 | 4.147038 | 2.366432 | 0.217424 | 4.189517 |
| Love | 4 | 2.366432 | 0.224487 | 4.123866 | 2.366432 | 0.222856 | 4.147468 | 2.366432 | 0.219779 | 4.190030 |
| Sanders | 4 | 2.366432 | 0.209964 | 4.124631 | 2.366432 | 0.205284 | 4.148371 | 2.366432 | 0.194994 | 4.191162 |
| Flügge | 4 | 2.366678 | 0.210024 | 4.123441 | 2.366723 | 0.205410 | 4.147025 | 2.366802 | 0.195325 | 4.189557 |

[a] Indicates imaginary frequencies.

$$G_n^{(2)} = (\alpha_{11} - \Omega^2)D_n + \alpha_{12}D_{n-2} + \alpha_{13}D_{n+2} + \alpha_{14}D_{n-4} + \alpha_{15}D_{n+4} + \alpha_{16}E_n + \alpha_{17}E_{n-2} + \alpha_{18}E_{n+2} + \alpha_{19}E_{n-4} + \alpha_{20}E_{n+4} + \alpha_{21}E_{n-6} + \alpha_{22}E_{n+6} \tag{19a}$$

$$G_n^{(3)} = \alpha_{26}D_n + \alpha_{27}D_{n-2} + \alpha_{28}D_{n+2} + \alpha_{29}D_{n-4} + \alpha_{30}D_{n+4} + \alpha_{31}D_{n-6} + \alpha_{32}D_{n+6} + (\alpha_{33} - \Omega^2)E_n + \alpha_{34}E_{n-2} + \alpha_{35}E_{n+2} + \alpha_{36}E_{n-4} + \alpha_{37}E_{n+4} + \alpha_{38}E_{n-6} + \alpha_{39}E_{n+6} + \alpha_{40}E_{n-8} + \alpha_{41}E_{n+8} \tag{19b}$$

Moreover, $H_n^{(j)}$ $(j=1,2,3)$ is obtained from $G_n^{(j)}$ $(j=1,2,3)$ by replacing $A$ with $B$, $D$ with $C$, $E$ with $F$, and $\alpha_i$ with $b_i$ $(i=1,2,\ldots,4)$. The parameters $\alpha_i$ and $b_i$ are obtained from those given in the Appendix of Ref. 1 by letting $\lambda_m \to 0$. In order that the homogeneous equations (16) and (17) vanish for any value of $s$, the coefficients of the linearly independent cos$ns$ and sin$ns$ terms must vanish. Thus,

$$G_n^{(1)} = 0, \quad H_n^{(1)} = 0, \text{ and } G_n^{(j)} = 0, \quad H_n^{(j)} = 0 \quad j = 2,3 \tag{20}$$

In Eqs. (20) $G_n^{(1)} = 0$ involves only the coefficients $A_n$, whereas $G_n^{(j)} = 0$ $(j=2,3)$ involves only the coefficients $D_n$ and $E_n$. Moreover, $H_n^{(1)} = 0$ involves only the coefficients $B_n$, whereas $H_n^{(j)} = 0$ $(j=2,3)$ involves only the coefficients $C_n$ and $F_n$. Thus, two independent solutions are obtained: one involving only the coefficients $A_n$, $D_n$, and $E_n$ and the other only the coefficients $B_n$, $C_n$, and $F_n$. The first solution is symmetric with respect to the $Y$ axis (see Fig. 1), while the second solution involves components of displacement $u$ and $w$ (which are antisymmetric with respect to the $Y$ axis). Moreover, $G_n^{(j)} = 0$ or $H_n^{(j)} = 0$ $(j=1,2,3)$ involve only either the odd or the even Fourier coefficients. Consequently, the coefficients $A_n$, $D_n$, $E_n$ or $B_n$, $C_n$, $F_n$ can be determined separately for odd or even values of $n$. It can be shown that the Fourier coefficients for even or odd values of $n$ are associated with components of displacement $w$, which are symmetric or antisymmetric respectively with respect to the $x$ axis (see Fig. 1). On this basis, it is apparent that the Fourier coefficients of the series expansions for the components of displacement [Eq. (3)] are divided into four groups, each associated with one of the four types of modes shown in Fig. 1. The Fourier coefficients belonging to the same group can be obtained from two different infinite sets of homogeneous equations that involve the frequency parameter $\Omega^2$. The one set represents longitudinal motion and the other plane strain motion.

In order to establish the frequencies and corresponding mode shapes, the Fourier series expansions of Eqs. (3) are truncated, retaining only as many terms as required in order that the frequencies and corresponding mode shapes are established within the desired accuracy. This leads to eight typical algebraic eigenvalue problems from which the four groups of SS, AS, SA, and AA modes (see Fig. 1) are obtained for both the purely longitudinal and plane strain modes.

## Numerical Results

Numerical results obtained on the basis of the Donnell, Love, Sanders, and Flügge types of theories are presented in Table 1. It is apparent that the frequencies of longitudinal vibrations obtained on the basis of Donnell, Love, and Sanders theories [Eqs. (14)] differ negligibly from those obtained on the basis of the Flügge-type theory. However, the frequencies of the lower plane strain modes obtained on the basis of the Donnell, Love, and Sanders theories differ appreciably from those obtained on the basis of the more accurate Flügge-type theory. The percent difference decreases as the number of circumferential nodes increases. The frequencies of oval shells ($\epsilon \neq 0$) vibrating in the lowest flexural mode ($n=1$) obtained of the basis of the Sanders-type theory are either imaginary or highly inaccurate.

## Reference

[1]Koumousis, V. K. and Armenàkas, A. E., "Free Vibrations of Simply Supported Cylindrical Shells," *AIAA Journal*, Vol. 21, July 1983, pp. 1017-1027.